

7-10-2003

# Determining the $\text{Ce}_2\text{O}_2\text{S}$ - $\text{CeO}_x$ Phase Boundary for Conditions Relevant to Adsorption and Catalysis

Robert M. Ferrizz  
*University of Pennsylvania*

Raymond J. Gorte  
*University of Pennsylvania, gorte@seas.upenn.edu*

John M. Vohs  
*University of Pennsylvania, vohs@seas.upenn.edu*

---

Postprint version. Published in *Applied Catalysis B: Environmental*, Volume 43, Issue 3, 10 July 2003, pages 273-280.  
Publisher URL: [http://dx.doi.org/10.1016/S0926-3373\(02\)00323-5](http://dx.doi.org/10.1016/S0926-3373(02)00323-5)

This paper is posted at Scholarly Commons. [http://repository.upenn.edu/cbe\\_papers/41](http://repository.upenn.edu/cbe_papers/41)  
For more information, please contact [repository@pobox.upenn.edu](mailto:repository@pobox.upenn.edu).

**Determining the Ce<sub>2</sub>O<sub>2</sub>S-CeO<sub>x</sub> Phase Boundary for Conditions  
Relevant to Adsorption and Catalysis**

by

R.M. Ferrizz, R.J. Gorte, and J.M. Vohs

Department of Chemical and Biomolecular Engineering  
University of Pennsylvania  
Philadelphia, PA 19104

**Abstract**

The interaction of sulfur with ceria under highly reducing conditions was investigated. The phase boundary between CeO<sub>1.83</sub> and Ce<sub>2</sub>O<sub>2</sub>S was determined for temperatures between 873 and 1073 K. This data was used to derive an empirical equation for  $\Delta G_f^\circ$  of Ce<sub>2</sub>O<sub>2</sub>S in this temperature range. This equation along with thermodynamic data for cerium oxides and sulfides obtained from the literature was used to predict Ce-O-S phase diagrams at 873 and 973 K. These phase diagrams provide insight into the mechanism of the deactivation of ceria-based catalysts by sulfur under reducing conditions.

## Introduction

Understanding the interaction of sulfur with ceria is important in a variety of applications where ceria is used as a catalyst, catalyst support, or sorbent [1-6]. These applications range from automotive emissions control to sulfur removal from fuels and flue gasses, to solid oxide fuel cells. For example, in the three-way automotive emissions control catalyst ceria is used to provide oxygen storage capacity, which increases the range of air-to-fuel ratios in which the catalyst can operate. Exposure of ceria to even small amounts of sulfur-containing compounds significantly decreases ceria's oxygen storage capacity [1, 7, 8] and the overall catalyst performance. This deleterious effect of sulfur on ceria is one of the prime driving forces for recently enacted government regulations in both the United States and Europe that mandate substantial reduction in fuel sulfur content.

We have recently shown that ceria is an excellent hydrocarbon oxidation catalyst for use in the anode of a solid oxide fuel cell. Composite anodes composed of mixtures of Cu, CeO<sub>2</sub>, and yttria-stabilized zirconia (YSZ) have been shown to be active for the direct electrochemical oxidation of hydrocarbons and highly resistant to fouling via carbon deposition [9-12]. This is in contrast to the more commonly used Ni/YSZ cermet anodes that rapidly deactivate due to coke deposition when exposed to dry hydrocarbons. As is the case for automotive catalysts, ceria-based SOFC anode catalysts are also affected by sulfur impurities in the fuel. This is illustrated by the data of Kim et al. [13] in Figure 1 which displays the current output at 0.5 V for a SOFC with a Cu/Ceria anode while operating on a fuel gas composed of 50 mol % decane in N<sub>2</sub> before and after the addition of 5000 ppm of S to the fuel. While operating on the decane/N<sub>2</sub> mixture the cell

exhibits stable operation. Introduction of 5000 ppm of sulfur, however, produces a 50 % decrease in the current output. It has been shown that this decrease is due to poisoning of the oxidation activity of the ceria.

Under oxidizing conditions, sulfur reacts with ceria to form cerium sulfates [4, 14]. In the case of automotive catalysts it is commonly thought that sulfate formation reduces the ability of the ceria to manage the oxygen partial pressure in the catalytic converter [1]. It is important to note, however, that while sulfates undoubtedly play a role in the deactivation of ceria under oxidizing conditions, different sulfur containing compounds may be formed under reducing conditions [5, 6, 15-17]. A detailed knowledge of cerium-sulfur chemistry under reducing conditions is therefore needed in order to fully understand sulfur deactivation of ceria. This is especially true in the applications mentioned above. During operation an automotive catalytic converter rapidly oscillates between oxidizing and reducing conditions. The gas exposed to the anode in a SOFC is also highly reducing.

In order to provide a more detailed understating of sulfur deactivation of ceria, especially under reducing conditions, we have recently used TPD, FTIR, and XPS to study the reaction of sulfur with ceria [15, 16]. These and other studies [1, 18, 19] show that SO<sub>2</sub> poisoning of ceria involves the formation of a complex set of compounds. As expected, under oxidizing conditions SO<sub>2</sub> reacts with ceria to form sulfates and sulfites. In contrast, under reducing conditions oxysulfides are formed. The inter-conversion between these various species upon changing the gas environment also appears to be rather facile. This complexity can be understood by considering a Ce-O-S phase diagram. Figure 2 displays the Ce-O-S phase diagram at 1100 K reported by Kay et al.

[20]. This phase diagram is based, for the most part, on free energies of formation that were measured at temperatures above 1100 K [20-23]. The phase diagram shows that for  $P_{O_2} > 0.1$  atm,  $Ce_2(SO_4)_3$  is the only stable sulfur containing species. Under more reducing conditions, the situation is much more complex and depending on the  $P_{S_2}$  cerium oxysulfide ( $Ce_2O_2S$ ) and various cerium sulfides ( $CeS$ ,  $Ce_3S_4$ , and  $Ce_2S_3$ ) can be formed.

From the perspective of using ceria-based catalysts under reducing conditions, the most important part of the phase diagram displayed in Figure 2 is the boundary between the cerium oxides and the cerium oxysulfide. This boundary in effect defines the  $P_{S_2}$  at which sulfur poisoning of ceria would be expected to occur. The temperature of this phase diagram, 1100 K, is at the upper end of the range that is of interest for most applications that make use of ceria catalysts. Thus, it is important to examine the Ce-O-S phase diagram at lower temperatures.

Kay et al. have compiled the necessary free energy and heat capacity data to allow one to calculate the Ce-O-S phase diagram at lower temperatures [20]. This data is listed in Table 1. Note that the most uncertain values in the table are those for  $Ce_2O_2S$ . The values for  $\Delta H_f^\circ$ ,  $S^\circ$  and  $C_p$  for this compound have not been measured directly. The values reported in the table for  $S^\circ$  and  $C_p$  are a weighted average of those for  $Ce_2O_3$  and  $Ce_2S_3$  [20] and the value for  $\Delta H_f^\circ$  of  $Ce_2O_2S$  was chosen to be consistent with that measured by Dwiendi and Kay at 1072 K [21]. In light of this, the uncertainty in the phase boundary between  $Ce_2O_2S$  and  $CeO_x$  is quite large when this data is used to predict phase diagrams at temperatures below 1072 K. This is unfortunate since this phase boundary is critical in predicting the effect of sulfur on the performance of ceria-based

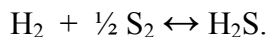
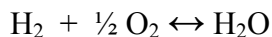
catalysts under reducing conditions. The motivation for the work described in this paper was, therefore, to examine the phase boundary between cerium oxides and cerium oxysulfide as a function of temperature for  $O_2$  and  $S_2$  partial pressures in ranges of interest for applications using ceria-based catalysts.

### **Experimental Methodology**

Phase diagrams based on the data reported by Kay et al. [20] were used as a guide to estimate  $P_{S_2}$  and  $P_{O_2}$  values which correspond to conditions near the cerium oxide-cerium oxysulfide phase boundary for temperatures between 873 and 1073 K. The formation, or lack thereof, of the oxysulfide for these conditions was then determined. This was done by annealing a  $CeO_2$  sample in a flowing gas stream with known values of  $P_{S_2}$  and  $P_{O_2}$  at the desired temperature. After equilibrium between the solid and gas phases had been established, temperature programmed oxidation (TPO) was used to determine if bulk  $Ce_2O_2S$  had been formed.

The experiments were carried out using a small flow reactor, which was contained in a tube furnace. The reactor was attached to a gas handling system that was equipped with mass flow controllers and allowed for the mixing of up to four individual gas streams. The specific gasses connected to the system in this study were He,  $O_2$ ,  $H_2$ , and 1030 ppm  $H_2S$  in He. Water was introduced into the gas stream by flowing He through a bubbler containing  $H_2O$ . During an experiment, the gas handling system was used to flow a gas with known partial pressures of He,  $H_2$ ,  $H_2O$  and  $H_2S$  through the reactor containing the ceria sample. The partial pressures of  $O_2$  and  $S_2$  in the reactor were

determined by assuming that the following reactions were in equilibrium inside the reactor:



The thermodynamics of the formation of  $\text{Ce}_2\text{O}_2\text{S}$  was studied for temperatures of 873, 973 and 1073 K.

In a typical experiment the  $\text{CeO}_2$  sample was initially pre-treated by heating to 973 K in a flowing stream of 10 mole %  $\text{O}_2$  in He and then annealed for five minutes at this temperature in 10 mole %  $\text{H}_2$  in He. The sample was then exposed to a flowing stream of He,  $\text{O}_2$ ,  $\text{H}_2$ , and  $\text{H}_2\text{S}$  and held at the desired temperature until equilibrium had been established. **Based on a study of the of the composition of the sample as a function of annealing time for conditions in which  $\text{Ce}_2\text{O}_2\text{S}$  was formed, it was determined that an annealing time of one hour was sufficient in order to obtain the equilibrium composition.** After annealing sample was then rapidly quenched to approximately 620 K in flowing He.

After quenching, TPO was used to determine the composition of the sample. During a TPO run the sample was heated to 1173 K with a linear temperature ramp of 20 K/min in a flowing stream of 10 mole %  $\text{O}_2$  in He. A small portion of the effluent from the reactor was admitted into a vacuum system containing a mass spectrometer, which was used to identify reaction products. For samples that contained sulfur,  $\text{SO}_2$  was produced in a sharp peak centered at 1100 K. An example of this is shown in curve A in Figure 3, which was obtained from a ceria sample that had been exposed to  $10^{-7}$  and  $10^{-20.4}$  atm of  $\text{S}_2$  and  $\text{O}_2$ , respectively at 1073 K. Curve B in this figure corresponds to

SO<sub>2</sub> desorption from a ceria sample that was exposed to 10<sup>-8</sup> and 10<sup>-20.6</sup> atm of S<sub>2</sub> and O<sub>2</sub>, respectively at 1073 K. Note that this latter treatment did not result in the production of the oxysulfide and the SO<sub>2</sub> desorption curve is flat.

The available thermodynamic data indicate that for the conditions used in this study the only sulfur-containing compound that should be formed is Ce<sub>2</sub>O<sub>2</sub>S. It is possible, however, that the thermodynamics of the formation of surface sulfide species may be different than that for bulk Ce<sub>2</sub>O<sub>2</sub>S. Quantification of the TPO SO<sub>2</sub> desorption peak was, therefore, used to determine if bulk Ce<sub>2</sub>O<sub>2</sub>S was indeed formed. This required a calibration factor for the SO<sub>2</sub> peak area. This calibration factor was measured by performing a TPO experiment with a known amount of Ce(SO<sub>4</sub>)<sub>2</sub> using the same flow rate of the O<sub>2</sub>/He mixture that was used in the TPO experiments with O<sub>2</sub>/S<sub>2</sub>-exposed ceria samples. During TPO with the Ce(SO<sub>4</sub>)<sub>2</sub> sample, SO<sub>2</sub> was also produced at 1100 K. The calibration factor for the SO<sub>2</sub> peak was determined by dividing the area of this peak by the number of moles of sulfur in the Ce(SO<sub>4</sub>)<sub>2</sub> sample. Based on quantification of the amount of SO<sub>2</sub> produced during TPO it was determined that the molar Ce:S ratio in all of the O<sub>2</sub>/S<sub>2</sub>-treated ceria samples that exhibited SO<sub>2</sub> peaks during TPO was approximately 2:1 which is consistent with the formation of bulk Ce<sub>2</sub>O<sub>2</sub>S.

## Results and Discussion

Figure 4 displays a portion of the Ce-O-S phase diagram for P<sub>O<sub>2</sub></sub> between 10<sup>-40</sup> and 10<sup>-20</sup> atm and P<sub>S<sub>2</sub></sub> between 10<sup>-30</sup> and 1 atm at 1073 K which is based on the data in Table 1. Since Kay et al. [20, 21] measured ΔG<sub>f</sub> for Ce<sub>2</sub>O<sub>2</sub>S at 1073 K, the phase boundary between Ce<sub>2</sub>O<sub>2</sub>S and the various cerium oxides at this temperature should be



fairly accurate. Note that in addition to  $\text{CeO}_2$  and  $\text{Ce}_2\text{O}_3$  the phase diagram contains  $\text{CeO}_{1.72}$  and  $\text{CeO}_{1.83}$ . As discussed in a recent review by Mogensen et al. [24] there is some data in the literature that indicates that other cerium sub-oxide phases may exist in this region of the phase diagram. Unfortunately, the stoichiometries of these other phases have yet to be unambiguously determined. Since the free energies of formation and the heat capacities of these additional phases should fall between those for  $\text{CeO}_2$  and  $\text{Ce}_2\text{O}_3$ , as do those for  $\text{CeO}_{1.72}$  and  $\text{CeO}_{1.83}$ , the inclusion of these additional phases would have little effect on the location of the phase boundary between  $\text{Ce}_2\text{O}_2\text{S}$  and  $\text{CeO}_x$ .

The data points in the figure were measured in the present study using the procedure described above. The circles and triangles correspond to conditions for which the TPO results showed the formation of  $\text{Ce}_2\text{O}_2\text{S}$ , and cerium oxide, respectively. Note that the data points collected in this study are consistent with the phase boundary between  $\text{Ce}_2\text{O}_2\text{S}$  and  $\text{CeO}_{1.83}$  predicted by the thermodynamic data reported by Kay et al. [20]. This is an important result and provides a verification of the experimental methodology used in the present study.

Figures 5 and 6 display Ce-O-S phase diagrams based on the thermodynamic data in Table 1 for reducing conditions and temperatures of 973 and 873 K. The individual data points in the figures were measured in the present study with the circles and triangles again corresponding to conditions for which the TPO showed the formation of  $\text{Ce}_2\text{O}_2\text{S}$ , and cerium oxides, respectively. The equilibrium phase boundary between  $\text{Ce}_2\text{O}_2\text{S}$  and  $\text{CeO}_{1.83}$  can be estimated based on the experimental data points. The data shows that the phase boundary at 973 K occurs at  $\text{S}_2$  partial pressures that are approximately one order of magnitude higher than those predicated by the thermodynamic data in Table 1. As

shown in Figure 6, at 873 K this phase boundary occurs at S<sub>2</sub> partial pressures that are approximately three orders of magnitude higher than those predicated by the thermodynamic data in Table 1.

Fitting values of  $\Delta G_f$  for Ce<sub>2</sub>O<sub>2</sub>S that were determined using the estimated values for  $\Delta H_f^\circ$ , S° and C<sub>p</sub> reported by Kay et al. [20] in Table 1 to a function of temperature results in the following equation:

$$\Delta G_f = -0.32 T - 1574.5 \quad \text{for} \quad 673 \text{ K} < T < 1073 \text{ K} \quad (1)$$

( $\Delta G_f$  [=] kJ/mol, T [=] K, reference states: pure components at 298 K and 1 atm)

As noted above, the data in Figures 5 and 6 show that this equation over estimates the magnitude of the free energy of formation for the oxysulfide. The phase boundary between Ce<sub>2</sub>O<sub>2</sub>S and CeO<sub>1.83</sub> determined experimentally can be used to provide a more accurate estimate of  $\Delta G_f$  for Ce<sub>2</sub>O<sub>2</sub>S as a function of temperature. Fitting of this data gives rise to the following equation for  $\Delta G_f$ :

$$\Delta G_f = -0.43 T - 1456.9 \quad \text{for} \quad 873 \text{ K} < T < 1073 \text{ K} \quad (2)$$

( $\Delta G_f$  [=] kJ/mol, T [=] K, reference states: pure components at 298 K and 1 atm)

The dotted lines in Figures 5 and 6 correspond to the phase boundaries between Ce<sub>2</sub>O<sub>2</sub>S, Ce<sub>2</sub>S<sub>3</sub> and the various cerium oxides that were calculated using values of  $\Delta G_f$  of Ce<sub>2</sub>O<sub>2</sub>S from equation 2. At least over this limited temperature range, these phase boundaries should be more accurate than those predicted using the data of Kay et al. [20].

The calculated Ce-O-S phase diagrams displayed in Figures 4 through 6 provide a useful starting point for understanding the effect of sulfur on ceria-based catalysts under reducing conditions. For example, they provide insight into the fuel cell performance data presented in Figure 1. In this example the power output of the fuel cell at 973 K while operating on a fuel composed of 50 mole % n-decane in N<sub>2</sub> decreased by approximately 50 % upon the addition of 5000 ppm of sulfur. Based on the overall fuel conversion and assuming equilibrium in the gas phase, the partial pressures of O<sub>2</sub> and S<sub>2</sub> in the cell were estimated to be 10<sup>-25.5</sup> and 10<sup>-12.6</sup> atm, respectively [13]. These conditions correspond to the diamond displayed in Figure 5. Note that this datum point falls within the Ce<sub>2</sub>O<sub>2</sub>S region of the phase diagram. This indicates that the decrease in performance upon the introduction of 5000 ppm sulfur was due to the formation of the oxysulfide.

The phase diagram also suggests that the ceria catalyst should not be seriously affected at more modest sulfur levels in the fuel. Indeed this has been experimentally verified and an identical fuel cell showed no performance degradation when 100 ppm of sulfur was added to a 5 mole % n-decane in N<sub>2</sub> fuel while operating at 973 K [13]. The calculated P<sub>O<sub>2</sub></sub> and P<sub>S<sub>2</sub></sub> in this case were 10<sup>-26.6</sup> and 10<sup>-20.3</sup> atm, respectively which correspond to the square in Figure 5. Note that this datum point falls in the CeO<sub>1.72</sub> region of the phase diagram.

These phase diagrams also have implications for the use of ceria in automotive exhaust catalysts. As noted above, the poisoning of ceria's oxygen storage capacity by sulfur is generally attributed to the formation of cerium sulfates [1, 7, 8]. Although this may be the case under oxidizing conditions, under reducing conditions other sulfur containing species such as the oxysulfide may be formed. Partial pressures of O<sub>2</sub> that are

low enough to result in oxysulfide formation are not likely to occur at the inlet to a catalytic converter even during fuel rich excursions. The  $P_{O_2}$  will obviously decrease significantly, however, down the length of the converter. Equilibrium calculations can be used to estimate a lower bound on the  $P_{O_2}$  that would be present in a catalytic converter under typical operating conditions during a fuel rich excursion. This type of calculation indicates that a  $P_{O_2}$  as low as  $10^{-30}$  atm is not unreasonable. Thus, the results of this study suggest that the formation of oxysulfides must be considered when assessing the effects of sulfur on the performance of three-way automotive catalysts.

## **Conclusions**

In this study the phase boundary between  $Ce_2O_2S$  and  $CeO_{1.83}$  was measured for temperatures between 873 and 1073 K. The location of this phase boundary was used to derive an empirical equation for  $\Delta G_f$  of  $Ce_2O_2S$  as a function of temperature. This equation along with thermodynamic data from the literature was used to calculate the equilibrium phase boundaries between the various cerium oxides,  $Ce_2O_2S$ , and  $Ce_2S_3$ . The calculated phase diagrams show that at temperatures between 673 and 1073 K, the formation of  $Ce_2O_2S$  requires significantly higher sulfur partial pressures than those suggested in previous studies. The Ce-O-S phase diagrams reported in this study provide a useful starting point for understanding the effect of sulfur on the performance ceria-based catalysts under reducing conditions

## **Acknowledgements**

This work was supported by the DARPA Palm Power Program.

## References

1. M. Boaro, C. de Leitenburg, G. Dolcetti, A. Trovarelli, M. Graziani, Topics in Catalysis 16 (2001) 299.
2. M. Flytzani-Stephanopoulos, Mrs Bull 26 (2001) 885.
3. Y. Zeng, S. Zhang, F. R. Groves, D. P. Harrison, Chem Eng Sci 54 (1999) 3007.
4. R. J. Gorte, T. Luo, Catalytic Science Series 2 (2002) 377.
5. M. Kobayashi, M. Flytzani-Stephanopoulos, Ind. Eng. Chem. Res. 41 (2002) 3115.
6. Z. Li, M. Flytzani-Stephanopoulos, Ind. Eng. Chem. Res. 36 (1997) 187.
7. D. D. Beck, J. W. Sommers, C. L. DiMaggio, Appl. Catal. B-Environ. 11 (1997) 273.
8. D. D. Beck, J. W. Sommers, C. L. Dimaggio, Appl. Catal. B-Environ. 3 (1994) 205.
9. R. J. Gorte, H. Kim, J. M. Vohs, J Power Sources 106 (2002) 10.
10. S. Park, R. J. Gorte, J. M. Vohs, Appl. Catal. A-Gen. 200 (2000) 55.
11. S. D. Park, J. M. Vohs, R. J. Gorte, Nature 404 (2000) 265.
12. H. Kim, S. Park, J. M. Vohs, R. J. Gorte, J. Electrochem. Soc. 148 (2001) A693.
13. H. Kim, J. M. Vohs, R. J. Gorte, Chem. Commun. 2001) 2334.
14. M. Waqif, P. Bazin, O. Saur, J. C. Lavalley, G. Blanchard, O. Touret, Appl. Catal. B-Environ. 11 (1997) 193.
15. T. Luo, J. M. Vohs, R. J. Gorte, J. Catal. 210 (2002) 397.
16. R. M. Ferrizz, R. J. Gorte, J. M. Vohs, Catal. Lett. in press (2002).
17. Y. Zeng, S. Kaytakoglu, D. P. Harrison, Che. Eng. Sci. 55 (2000) 4893.
18. J. A. Rodriguez, T. Jirsak, A. Freitag, J. C. Hanson, J. Z. Larese, S. Chaturvedi, Catal. Lett. 62 (1999) 113.

19. S. H. Overbury, D. R. Mullins, D. R. Huntley, L. Kundakovic, J. Phys. Chem. B 103 (1999) 11308.
20. D. A. R. Kay, W. G. Wilson, V. Jalan, J Alloy Compd 193 (1993) 11.
21. R. K. Dwivedi, D. A. R. Kay, J Less-Common Met 102 (1984) 1.
22. I. Barin, O. Knacke, Thermochemical Properties of Inorganic Substances, Springer-Verlag, New York, 1973, .
23. I. Barin, O. Knacke, Thermochemical Properties of Substances - Supplement, Springer-Verlag, New York, 1977, .
24. M. Mogensen, N. M. Sammes, G. A. Tompsett, Solid State Ionics 129 (2000) 63.

## Figure Captions

Figure 1. Performance of a SOFC as a function of time at 973 K while holding the cell potential at 0.5 V [8]. During the first two hours the feed to the anode was 50 mole % n-decane in N<sub>2</sub> and then 5000 ppm of sulfur was added to the fuel.

Figure 2. Ce-O-S phase diagram at 1100 K based on the data in Table 1.

Figure 3. Sulfur dioxide desorption curves during TPO from samples that were previously treated in (A) 10<sup>-7</sup> and 10<sup>-20.4</sup> atm of S<sub>2</sub> and O<sub>2</sub>, respectively at 1073 K and (B) 10<sup>-8</sup> and 10<sup>-20.6</sup> atm of S<sub>2</sub> and O<sub>2</sub>, respectively at 1073 K.

Figure 4. Ce-O-S phase diagram at 1073 K based on the data in Table 1. The data points in the figure were measured in the present study. The circles and triangles correspond to conditions for which Ce<sub>2</sub>O<sub>2</sub>S, and cerium oxide are stable, respectively.

Figure 5. Ce-O-S phase diagram at 973 K based on the data in Table 1. The data points in the figure were measured in the present study. The circles and triangles correspond to conditions for which Ce<sub>2</sub>O<sub>2</sub>S, and cerium oxide are stable, respectively. The dotted lines are based on the  $\Delta G_f$  of Ce<sub>2</sub>O<sub>2</sub>S measured in the present study.

Figure 6. Ce-O-S phase diagram at 873 K based on the data in Table 1. The data points in the figure were measured in the present study. The circles and triangles correspond to conditions for which  $\text{Ce}_2\text{O}_2\text{S}$ , and cerium oxide are stable, respectively. The square and diamond data points were obtained in a study of the effect of sulfur on the performance of a SOFC and are described in the text. The dotted lines are based on the  $\Delta G_f$  of  $\text{Ce}_2\text{O}_2\text{S}$  measured in the present study.